Published online 25 March 2016

Nucleic Acids Research, 2016, Vol. 44, No. 8 ***3495–3502***
doi: 10.1093/nar/gkw200

Direct and site-specific quantification of RNA 2′-O-methylation by PCR with an engineered DNA polymerase

Joos Aschenbrenner and Andreas Marx*

Department of Chemistry, Konstanz Research School Chemical Biology, University of Konstanz, Universitätsstraße 10, D-78457 Konstanz, Germany

Received February 17, 2016; Revised March 11, 2016; Accepted March 14, 2016

ABSTRACT

Methylation of the 2′-hydroxyl-group of ribonucleotides is found in all major classes of RNA in eukaryotes and is one of the most abundant posttranscriptional modifications of stable RNAs. In spite of intense studies, the multiple functions of RNA 2′-O-methylation are still not understood. One major obstacle in the field are the technical demanding detection methods, which are typically laborious and do not always deliver unambiguous results. We present a thermostable KlenTaq DNA polymerase variant with significant reverse transcription activity that is able to discriminate 2′-O-methylated from unmethylated RNAs. The engineered enzyme catalyzes DNA synthesis from DNA as well as RNA templates and enables expeditious quantification of 2′-O-methylation of individual nucleotides directly from total RNA extracts by a simple qRT-PCR.

INTRODUCTION

Modified nucleotides are a ubiquitous feature of life and provide an increased diversity of cellular DNA and RNA. In particular, cellular RNAs contain a large variety of modifications, which are usually introduced by posttranscriptional modification (1,2). To date, more than 100 chemically distinct RNA modifications have been identified in Bacteria, Archaea and Eukarya (3,4). One of the most abundant modifications of RNA is methylation of the 2′-hydroxyl group of the ribose moiety. 2′-O-methylated nucleotides are present in all major classes of eukaryotic RNA, but are best-studied in rRNA. In the human ribosome more than 100 2′-O-methylation sites have been mapped (5,6). Site specific 2′-O-methylation of eukaryotic rRNA is mainly guided by numerous small nucleolar RNAs (snoRNAs), which direct the enzymatic machinery required for methylation toward complementary target regions in the ribosome (7). Those modification sites are highly conserved among vertebrates and mainly occur clustered in functionally important regions, where they are very likely to modulate biogenesis and activity of the ribosome (8). However, the detailed function of 2′-O-methylation in rRNA is not yet well understood. Modifications may fine-tune rRNA folding and a wide range of RNA–RNA and RNA–protein interactions by enhancing hydrophobic surfaces and stabilizing helical stem structures (7). Differential methylation patterns of ribosomes are proposed to be a potential source of heterogeneity that may confer regulatory control of translation through 'specialized ribosomes' (9). The fact that alterations or defects in ribosomal methylation are associated with heritable diseases and cancer leaves little doubt about its functional significance (10–12). The relevance of RNA-guided 2′-O-methylation of RNAs was further emphasized by the detection of snoRNAs that target other cellular RNAs, including snRNA, tRNAs and possibly even mRNAs for methylation (1,7,13,14). These findings revealed functional roles of 2′-O-methylation in splicing control (15) and further fundamental cellular processes. Evidently, many aspects of ribose methylation in RNAs still remain to be discovered. Methods to detect 2′-O-methylation in RNA utilize TLC, HPLC or LC-MS to analyze appropriately labeled RNAs after digestion with suitable endonucleases (16–18). These methods require large amounts of highly pure RNA and are very laborious and not suited to detect modifications in low-abundance RNAs. Different approaches exploit enhanced resistance toward alkaline hydrolysis (19) or differential enzymatic turn-over (20,21) of 2′-O-methylated RNA. For instance, the propensity of some reverse transcriptases to pause primer elongation at low dNTP concentrations when encountering 2′-O-methylation in the template has been used to find these modifications (22). Those methods do not require purification of RNA species and can be directly applied to total RNA extracts. However, the high labor intensity and, in some cases, the ambiguity of results still hamper RNA methylation analysis (23). We herewith present a conceptually new approach for a significantly simplified RNA methylation analysis. Our studies reveal a thermostable DNA polymerase which is able to utilize RNA

*To whom correspondence should be addressed. Tel: +49 7531 885139; Fax: +49 7531 885140; Email: andreas.marx@uni-konstanz.de

as well as DNA as template for DNA synthesis (24) and is able to discriminate 2′-O-methylated from unmethylated RNA. Based on these findings, we generated a DNA polymerase with improved discrimination properties and employed it in a methylation specific direct qRT-PCR assay. Along these lines, we were able to quantify the methylation status of five known methylation sites in human 18s rRNA from a variety of different human cancer cell lines by a simple one-step assay directly applied on total RNA extracts. These findings significantly reduce the complexity of 2′-O-methylation analysis. Our data also provide evidence for the occurrence of some ribosomal heterogeneity within human cell lines.

MATERIALS AND METHODS

Oligonucleotides and human total RNA

DNA Oligonucleotides were purchased from Biomers and were used directly for RT-PCR experiments, or purified by preparative denaturating PAGE for primer extension experiments. Radioactive labeling of primer strands was performed using [γ-^{32}P]-ATP and T4 polynucleotide kinase according to the vendor's protocol. RNA oligonucleotides were purchased from Purimex. The sequences of all used oligonucleotides are listed in Supplementary Table S1. Extraction of total RNA from human cell lines was achieved using the Direct-zol™ RNA MiniPrep Kit (Zymo Research) according to the vendor's protocol. In-column DNase treatment was performed by the addition of 20u DNase I per column and incubation at room temperature for 15 min. RNA concentration was determined using NanoDrop™ 1000 Spectrophotometer (PEQLAB). Determined A260/A280 values were ≥2.0. RNA integrity was analyzed by agarose gel electrophoresis and the 28s/18s rRNA ratio ranged from 1.7 to 2.1 (Supplementary Figure S1).

In vitro transcribed RNA

cDNA of the human 18s rRNA was obtained by reverse transcription from human RNA extracts using a suitable primer and M-MuLV Reverse Transcriptase (NEB) according to the vendor's protocol, and amplified by PCR employing Phusion® DNA polymerase (NEB). Amplified cDNA was purified via agarose gel electrophoresis. cDNA was cloned into a pJET 1.2 vector (Thermo), transformed into *E.coli* T7 express Iq (NEB) and checked for correct sequence by Sanger sequencing (GATC Biotech). Subsequently, correctly sequenced plasmid was isolated using QIAprep® Spin Miniprep Kit (Qiagen) and linearized by endonuclease digestion with ClaI (NEB). Linearized plasmid was purified by phenol-chloroform extraction and ethanol precipitation. *In vitro* transcription of the linearized plasmid was achieved using the HiScribe™ T7 High Yield RNA Synthesis Kit (NEB) according to the vendor's protocol. After digestion of the DNA template by addition of 4u DNase I (NEB) and incubation at 37°C for 15 min, *in vitro* transcribed RNA was purified by phenol-chloroform extraction and ethanol precipitation. Subsequently, RNA was dissolved in RNase-free water and RNA concentration was determined using NanoDrop™ 1000 Spectrophotometer (PEQLAB). A260/A280 was 2.4. Purity of the *in vitro* transcribed RNA was additionally analyzed by agarose gel electrophoresis (Supplementary Figure S1). For later usage, RNA was stored at −80°C.

Protein expression and purification

Protein expression was performed in *E.coli* BL21 DE3 (Novagen) as described (24). Purification of 6x His-tagged KlenTaq variants was achieved via heat denaturation of lysates at 75°C for 45 min, followed by ultracentrifugation at 20.000 rpm for 45 min and FPLC purification using a His-Trap FF crude column (GE HEALTHCARE) and a linear gradient from 5 to 500 mM imidazole (binding buffer: 100 mM Trizma® base (pH 9.2), 5 mM $MgCl_2$, 300 mM NaCl, 5 mM Imidazol; elution buffer: 100 mM Trizma® base (pH 9.2), 5 mM $MgCl_2$, 300 mM NaCl, 500 mM Imidazol). Enzymes were then concentrated by Vivaspin (Sartorius) and stored in storage buffer (50 mM Trizma base (pH 9.2), 2.5 mM $MgCl_2$, 16 mM $(NH_4)_2SO_4$, 0.1% (v/v) Tween, 50% (v/v) Glycerol) at −20°C. Purity of enzymes was validated by SDS-PAGE (Supplementary Figure S2).

RT-KTQ-LSIM library construction

All possible RT-KTQ-LSIM single mutants at the positions G668, V669, G672, R746, K747 and N750 were created by site directed mutagenesis of the respective codon. To obtain all 19 mutants at one site, 19 separate PCR reactions were performed respectively, each with the same 5′-phosphorylated reverse primer, but with an individual forward primer carrying the triplet coding for the destined amino acid. After PCR amplification employing Phusion® DNA polymerase and DpnI digestion of the template plasmid, reactions were purified using a NucleoSpin® Gel and PCR Clean-up (Macherey-Nagel). PCR products were ligated using T4 DNA ligase (NEB) and transformed into *E.coli* BL21 DE3 (Novagen). Plasmids were sequenced by Sanger sequencing (GATC Biotech) and clones carrying plasmids with correct RT-KTQ-LSIM mutants were cultured overnight in 700 µl LB-medium containing 100 µg/ml carbenicillin in 96 well deep-well plates at 37°C. Subsequently, 700 µl of 60% (v/v) glycerol in LB-medium was added and plates were stored at −80°C.

Screening for improved RT-KTQ mutants

RT-KTQ-LSIM variants were expressed in duplicates in 96 well plates. Harvested cells were resuspended in 1x KlenTaq reaction buffer (50 mM Trizma® base (pH 9.2), 16 mM $(NH_4)_2SO_4$, 2.5 mM $MgCl_2$, 0.1% (v/v) Tween) containing 0.5 mg/ml lysozyme, and lyzed by incubation at 37°C for 20 min. After denaturation of *E.coli* host proteins by incubation at 75°C for 45 min, plates were centrifuged at 4400 rpm and 4°C for 30 min and lysates were directly deployed in qRT-PCR (25). For this purpose, 10 µl lysate was mixed with 10 µl 2x Mastermix (400 µM dNTPs, 200 nM forward primer, 200 nM reverse primer, 100 mM betaine, 2x SYBR® green I (sigma), 100 nM Taq DNA polymerase

aptamer (26) and 200 pM RNA template in 1x KlenTaq reaction buffer) and analyzed by qRT-PCR, using a Roche Lightcycler® 96 instrument with the following protocol: 60s at 95°C; then 50 cycles of 15s at 95°C and 30s at 62°C. RT-KTQ-LSIM variants with improved discrimination of 2′-O-methylated and unmethylated template were expressed in a larger scale and purified before further characterization.

Primer extension assay with RNA oligonucleotides as template

The reaction mixture contained 150 nM of [γ-^{32}P]-labeled primer, 225 nM of the respective RNA template and 200 μM dNTPs (each) in 1x KlenTaq reaction buffer. Reaction mixtures (20 μl, respectively) were heated to 95°C for 2 min and subsequently cooled to 55°C. After starting the primer extension by addition of either 250 pM RT-KTQ-LSIM or 2.5 nM RT-KTQ-LSIM V669L, reactions were allowed to proceed at 55°C for 10 min. Reactions were stopped by addition of 40 μl stop solution (80% (v/v) formamide, 20 mM EDTA, 0.25% (w/v) bromophenol blue, 0.25% (w/v) xylene cyanol) and analyzed by 12% denaturating PAGE. Visualization was performed by phosphorimaging.

Specific Activity of RT-KTQ variants

Extension of primer in complex with the respective RNA template was performed as described above, analyzed by 12% denaturating PAGE and visualized via phosphorimaging. Reactions were performed with various amounts of DNA polymerase (RT-KTQ-LSIM: 0.25–100 fmol; RT-KTQ-LSIM V669L: 5–300 fmol) in 20 μl reaction mixture. The observed intensities of each band in the autoradiogram yielded the conversion of dNTPs in each reaction. dNTP conversion per min was plotted against the amount of applied enzyme. The linear range was analyzed and slopes were obtained by linear regression (Supplementary Figure S3), yielding the specific activity of the respective enzyme and the respective sequence context (27).

Primer extension assay with human RNA extracts/*in vitro* transcribed 18s rRNA as template

The reaction mixture contained 30 nM of [γ-^{32}P]-labeled primer, 200 μM dNTPs (each) and 200 ng/μl total RNA extracts or 80 ng/μl *in vitro* transcribed 18s rRNA in 1x KlenTaq reaction buffer. Reaction mixtures (20 μl, respectively) were heated to 95°C for 2 min and subsequently cooled to 55°C. After starting the primer extension by addition of 20 nM RT-KTQ-LSIM V669L, reactions were allowed to proceed at 55°C for 10 min. Reactions were stopped by addition of 40 μl stop solution (80% (v/v) formamide, 20 mM EDTA, 0.25% (w/v) bromophenol blue, 0.25% (w/v) xylene cyanol) and analyzed by 12% denaturating PAGE. Visualization was performed by phosphorimaging.

qRT-PCR using RNA oligonucleotides as template

qRT-PCRs were conducted in a total volume of 20 μl reaction mixture containing 100 pM RNA oligonucleotide, 100 nM forward primer, 100 nM reverse primer, 200 μM dNTPs (each), 0.5 M betaine, 1x SYBR® green I (sigma), 100 nM Taq Aptamer (26) and 100 nM of either RT-KTQ-LSIM or RT-KTQ-LSIM V669L in KlenTaq reaction buffer. qRT-PCR was conducted in triplicates using a Roche Lightcycler® 96 instrument with the following protocol: 60 s at 95°C; then 40 cycles of 15 s at 95°C and 30 s at 62°C. For Analysis of the RT-PCR by Agarose Gel electrophoresis, qRT-PCR was stopped after 25 (RNA template A and 2′OmeA) or 30 cycles (RNA template C and 2′OmeC), respectively. ΔC_T-values were used to calculate 2′-O-methylation fractions. Efficiency of the PCR was determined by template dilution series using the unmodified templates.

qRT-PCR with human RNA extracts and *in vitro* transcribed 18s rRNA

qRT-PCRs were conducted in a total volume of 20 μl reaction mixture containing 100 nM forward primer, 100 nM reverse primer, 200 μM dNTPs (each), 0.5 M betaine, 1x SYBR® green I (sigma), 100 nM Taq DNA polymerase aptamer (26) and 100 nM of either RT-KTQ-LSIM or RT-KTQ-LSIM V669L in KlenTaq reaction buffer. The concentrations of the different RNAs were adjusted for each site individually deploying the respective control primer sets, and ranged from 2.5 to 10 ng/μl for human RNA extracts and 0.5 to 2 ng/μl for *in vitro* transcribed RNA. qRT-PCR was conducted in triplicates using a Roche Lightcycler® 96 instrument. For the sites A27, U428, G1490 and C1703, the following protocol was applied: 60s at 95°C; then 40 cycles of 15 s at 95°C and 45 s at 60°C. For the site A99, the following protocol was applied: 60 s at 95°C, then 40 cycles of 15 s at 95°C, 30 s at 60°C and 5 s at 72°C (the additional extension step at 72°C was necessary to achieve specific amplification). To validate specific amplification, melting points of PCR products were measured (Supplementary Table S2). $\Delta\Delta C_T$-values were used to calculate 2′-O-methylation fractions (Supplementary Table S3). Efficiencies of the PCRs were determined by template dilution series of the *in vitro* transcribed 18s rRNA (Supplementary Figure S4). To exclude DNA contamination of the total RNA samples, a minus-reverse transcription control was conducted by PCR with a commercially available KlenTaq DNA Polymerase Mastermix (myPOLS Biotec), 0.5 M betaine, 1x SYBR® green I (sigma) and 5 ng/μl RNA sample. For all used primer sets, minus-reverse transcription PCRs harbored either only primer dimers or no product at all.

RESULTS

A KlenTaq variant with reverse transcriptase activity discriminates 2′-O-methylated from unmethylated RNA

First, we investigated a thermostable variant of KlenTaq (Klenow fragment of the *Thermus aquaticus* DNA polymerase) with reverse transcriptase activity (24) in its behavior when encountering 2′-O-methylation in an RNA template during primer elongation. The previously described KlenTaq L459M S515R I638F M747K mutant (24) (henceforth called RT-KTQ-LSIM) was employed to catalyze the

extension of a primer hybridized to different RNA oligonucleotides with identical sequence but carrying either a 2′-O-methylated nucleotide at the position of first incorporation or the respective unmodified one (Figure 1). We found that 2′-O-methylation is a major obstacle for reverse transcription catalyzed by RT-KTQ-LSIM even at dNTP concentrations of 200 μM and irrespective of the methylated nucleotide carrying a pyrimidine (C) or a purine (A) as nucleobase (Figure 1B). Since RT-KTQ-LSIM is a thermostable enzyme, we envisioned to exploit this discrimination in order to develop a methylation specific qRT-PCR system. Therefore, we applied the aforementioned primer/template combination and designed an appropriate forward primer which results in a PCR amplicon of 53 nt. As C_T-values of qRT-PCR experiments also depend on the concentration of the target RNA, we designed an additional reverse primer, which terminates several nucleotides downstream of the analyzed nucleobase, as a control (Figure 1C). Using this control reverse primer in combination with the same forward primer, should result in a qRT-PCR that is not impeded by methylation of the respective nucleotide. When using the methylation-specific primers, qRT-PCR did indeed result in a delayed amplification of methylated RNAs in comparison to the respective unmethylated ones, while amplification curves coincided when using the control primer sets. The discrimination was higher for a methylated cytidine in the template (average $\Delta C_T = 4.6$) than for a methylated adenosine (average $\Delta C_T = 1.9$).

Generation of an improved RT-KTQ variant

We aimed to generate RT-KTQ-LSIM variants with improved discrimination of 2′-O-methylated nucleotides. Therefore, we created libraries with single mutants of RT-KTQ-LSIM by site-directed mutagenesis. Mutation sites were selected by inspection of the crystal structure of RT-KTQ-LSIM in complex with DNA/RNA hybrid and a bound triphosphate (24) (Figure 2). Amino acids with close proximity to the 2′-O-hydroxyl of the ribonucleotide paired to the incoming dNTP (namely G668, V669, G672, R746, K747 and N750) were chosen for saturation mutagenesis. Libraries were screened for improved discrimination of 2′OmeA from unmethylated A directly from cell lysate (25), using the above-named qRT-PCR system. Mutants which exhibited increased ΔC_T-values between the respective templates were Ni-NTA purified and further analyzed by primer extension and qRT-PCR experiments. Best results were obtained with an RT-KTQ-LSIM V669L mutant featuring enhanced discrimination of 2′-O-methylated RNA in both, primer extension and qRT-PCR (Figure 3A–C). The ΔC_T-value did not only increase for the screened 2′OmeA/A discrimination (average $\Delta C_T = 7.7$), but also when comparing the methylated C template to the unmethylated one (average $\Delta C_T = 6.3$). By looking at the specific activity (27) of RT-KTQ-LSIM V669L and RT-KTQ-LSIM on unmethylated and methylated RNA templates, the improved properties of the mutant become evident. Albeit both enzymes exhibit differences between activities on methylated and unmethylated templates, these differences raise from ∼3.5-fold for RT-KTQ-LSIM to ∼7-fold for RT-KTQ-LSIM V669L (Table 1 and Supplementary Figure S3). Moreover, the ability of RT-KTQ-LSIM V669L to utilize these catalytic differences in qRT-PCR is enhanced due to its decreased activity on RNA, resulting in an increased limitation of the actual discriminating step, namely first strand synthesis by reverse transcription.

Direct quantification of RNA 2′-O-methylation by qRT-PCR

We hypothesized that qRT-PCR, catalyzed by RT-KTQ-LSIM V669L, could be evaluated in a quantitative manner to determine the fraction of 2′-O-methylation at a target site. Therefore, we mixed known ratios of a 2′-O-methylated RNA template with its unmethylated equivalent and measured ΔC_T values in reference to the fully unmethylated template. By approximation, we postulated that any amplification of the target derives from the unmethylated template only, enabling the calculation of the methylation fraction by the comparative C_T method (28):

$$methylation\ fraction = 1 - E^{-(\Delta C_{T\ methylation\ specific\ primers} - \Delta C_{T\ control\ primers})}$$

$$with\ E = PCR\ efficiency$$

This seems to be a valid assumption as a ΔC_T value of ∼7 cycles, as caused by RNA methylation, corresponds to a decrease of RNA concentration by two orders of magnitude, resulting in an error of only ∼1%. Our data confirm that this approach actually allows a very accurate estimation of the methylation fraction (Figure 3D). Next, we used this direct qRT-PCR assay to analyze the methylation fraction of five known methylation sites (namely A27, A99, U428, G1490 and C1703) in human 18s rRNA directly from total RNA extracts deriving from various immortalized and/or cancer cell lines. As unmodified reference RNA, we employed *in vitro* transcribed 18s rRNA. For each site, RNA concentrations were adjusted by qRT-PCR with a control primer terminating 5 or 6 nucleotides downstream of the methylation site. To analyze the methylation site, reverse primers were designed which directly terminate one nucleotide upstream of the analyzed nucleotide. Both reverse primers were combined with the same forward primer, delivering amplicons of ∼40–60 nt, which contain only one site of methylation (cf. Figure 1C). Our results show that most of the analyzed sites are methylated uniformly throughout different cell lines and methylation fractions range from 80% upward (Figure 4A, Supplementary Table S3). The methylation of A99, however, drops below 50% in colorectal cancer cells (Caco2) (Figure 4B). Inhomogeneity of A99 methylation was further verified by radioactive primer extension experiments catalyzed by RT-KTQ-LSIM V669L (Supplementary Figure S5).

DISCUSSION

In summary, we found that DNA synthesis by a KlenTaq DNA polymerase variant with reverse transcriptase activity is stalled by the presence of 2′-O-methylation in the RNA template and employed this effect in a methylation-sensitive qRT-PCR. These findings pave the way for a significantly

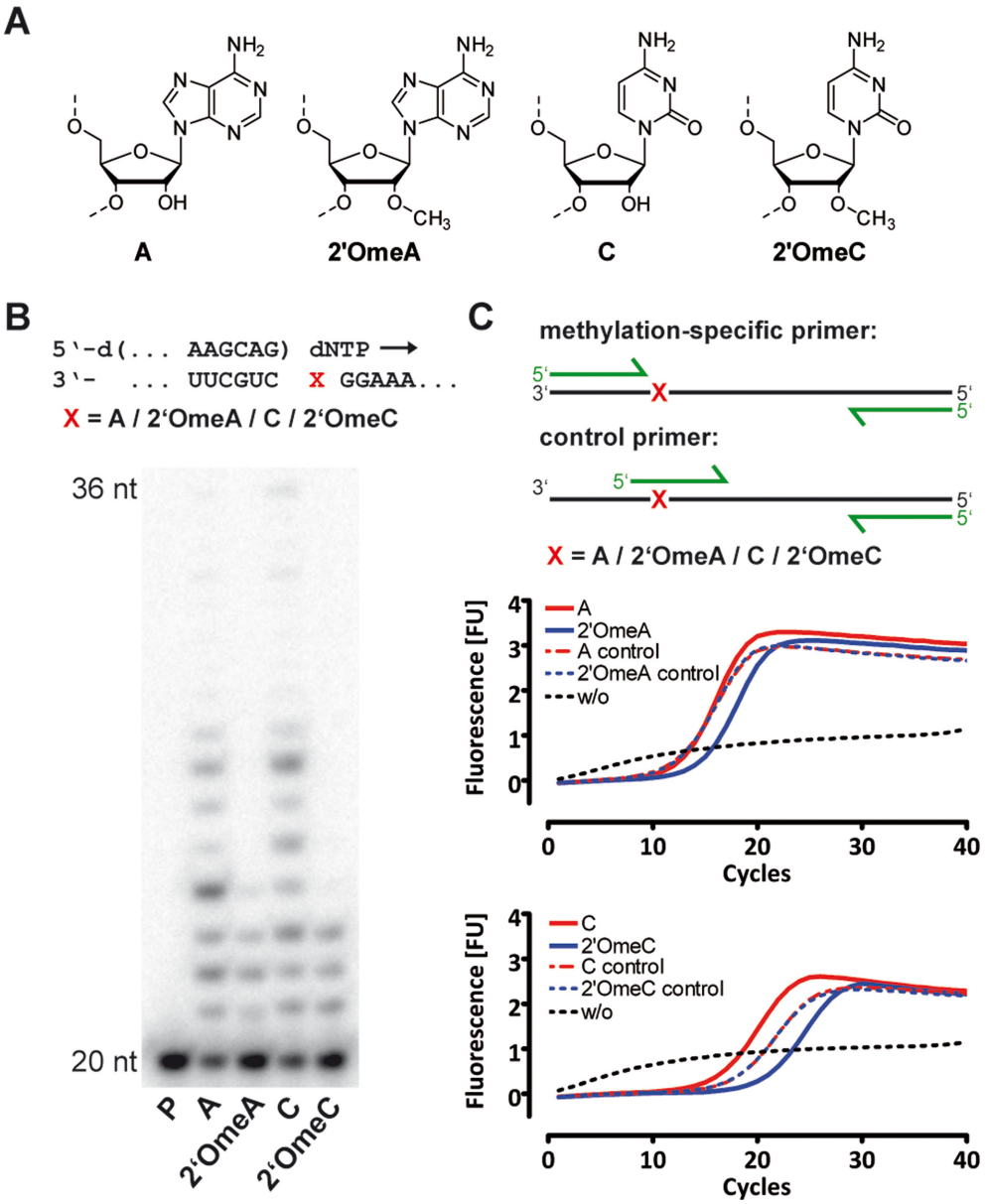

Figure 1. DNA synthesis catalyzed by RT-KTQ-LSIM is hampered by 2′-O-methylation of RNA templates. (**A**) Structures of relevant nucleotides. (**B**) Primer extension in presence of methylated or unmethylated RNA templates catalyzed by RT-KTQ-LSIM. (**C**) qRT-PCR amplification of methylated and unmethylated RNA oligonucleotides catalyzed by RT-KTQ-LSIM.

Table 1. Specific activity of RT-KTQ-LSIM variants on methylated and unmethylated templates

DNA polymerase	template	specific activity [min^{-1}]
RT-KTQ-LSIM	A	94.9 ± 1.8
RT-KTQ-LSIM	2′OmeA	30.5 ± 1.6
RT-KTQ-LSIM	C	120.9 ± 7.9
RT-KTQ-LSIM	2′OmeC	25.6 ± 1.4
RT-KTQ-LSIM V669L	A	22.1 ± 1.3
RT-KTQ-LSIM V669L	2′OmeA	3.17 ± 0.07
RT-KTQ-LSIM V669L	C	25.6 ± 1.1
RT-KTQ-LSIM V669L	2′OmeC	3.83 ± 0.08

Data points derive from triplicates. ± describes SD.

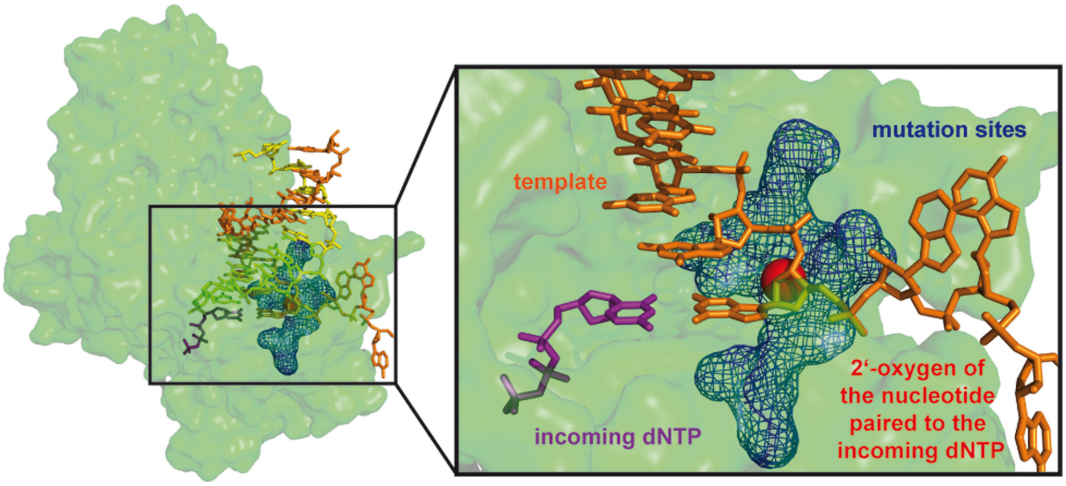

Figure 2. Rational design of RT-KTQ-LSIM libraries. Amino acids in immediate proximity to the 2′-oxygen of the nucleotide paired to the incoming dNTP were selected for saturation mutagenesis (namely G668, V669, G672, R746, K747 and N750). Adapted from PDB 4BWM (24) using PyMOL (Schrödinger, LLC, New York, NY, USA).

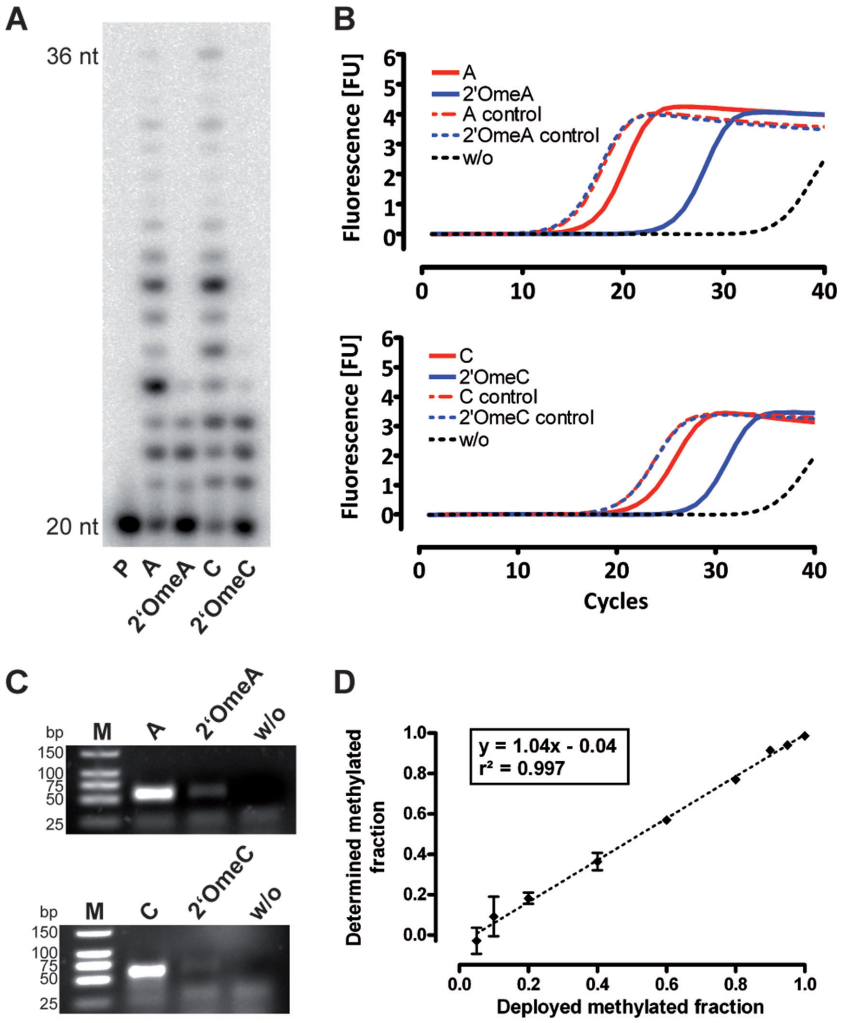

Figure 3. RT-KTQ-LSIM V669L features increased discrimination between 2′-O-methylated and unmethlyated RNA templates and enables quantification of 2′-O-methylation by qRT-PCR. (**A**) Primer extension in the presence of methylated or unmethlyated RNA templates catalyzed by RT-KTQ-LSIM V669L. (**B**) qRT-PCR amplification of methylated and unmethylated RNA oligonucleotides catalyzed by RT-KTQ-LSIM V669L. (**C**) RT-PCR reactions were stopped after 25 cycles (top) or 30 cycles (bottom) and analyzed by agarose gel electrophoresis. (**D**) The ΔC_T-method was used to calculate methylation ratio of RNA template at 100 pM concentration with varied fractions of 2′OmeA/A at the target position. Error bars describe SD (n = 3).

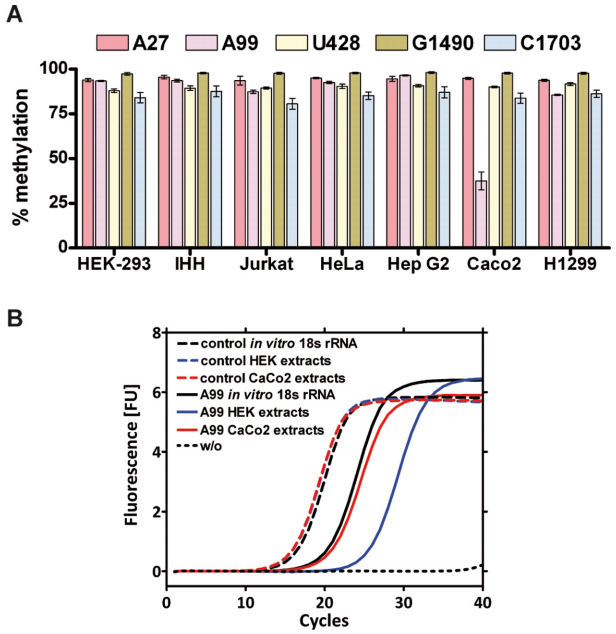

Figure 4. Quantification of ribosomal methylation directly from total RNA by qRT-PCR. (**A**) Analysis of the methylation status of A27, A99, U428, G1490 and C1703 in 18s rRNA from total RNA extracts of various human cell lines. Error bars describe SD. (**B**) qRT-PCR data of methylation site A99 in HEK-293 and Caco2 cells. ΔC_T values indicate higher degree of methylation in HEK-293 cells than in Caco2 cells.

simplified analysis of RNA modification with high sensitivity. The developed approach is capable of assessing the 2′-O-methylation fraction of individual nucleotides within 1 h in a high-throughput fashion and is sensitive for target RNAs at picomolar concentrations. Since both reaction steps of the assay—first strand synthesis by reverse transcription and amplification by PCR—are catalyzed by the same enzyme, qRT-PCR can be performed directly on total RNA extracts by simply adding a 'PCR mastermix' and running a conventional PCR protocol. The developed PCR-assay was successfully used to quantify the 2′-O-methylation-fraction of five known methylation sites in human 18s rRNA throughout different cell types. Our data display that the methylation fractions of the analyzed sites are mainly homogeneous. However, 2′-O-methylation of A99 was found to be significantly decreased in colon cancer cells, suggesting that this methylation site might serve as potential biomarker for some cancer cells. Interestingly, the homologous A100 in yeast 18s rRNA was also found to be only partially methylated using an LC-MS/MS based method (29). To improve the deployed RT-KTQ-LSIM DNA polymerase, we introduced an additional mutation. The mutation of V669 to the sterically slightly more demanding leucine is located in the O-helix (30) of the DNA polymerase and might influence the transition of the enzyme to a ternary complex closed conformation in which the reactive groups are aligned for catalysis in a way that is more favorable for unmodified RNA templates in comparison to 2′-O-methylated RNA. It has been reported that some DNA polymerases are able to also sense base modifications in their template (31,32). Hence, further enzyme engineering and screening of new DNA polymerase variants may open up this qRT-PCR-based approach for analysis of other biologically significant RNA modifications (33) in the future.

SUPPLEMENTARY DATA

Supplementary Data are available at NAR Online.

ACKNOWLEDGEMENT

We thank J. Demgenski and Prof. Dr T. Brunner (Department of Biology, University of Konstanz) for providing human cell lines and cell culture. We also thank D. Rösner (Department of Chemistry, University of Konstanz) and R. Kranaster (myPOLS Biotec) for helpful discussions. We gratefully acknowledge support by the Konstanz Research School Chemical Biology.

FUNDING

Deutsche Forschungsgemeinschaft [SPP 1784]; European Research Council [ERC Advanced Grant 339834]; Carl Zeiss Stiftung (stipend to J.A.). Funding for open access charge: Deutsche Forschungsgemeinschaft.
Conflict of interest statement. None declared.

REFERENCES

1. Grosjean,H. (2005) *Fine-tuning of RNA functions by modification and editing*. Springer-Verlag: Berlin, Heidelberg.
2. Limbach,P.A., Crain,P.F. and McCloskey,J.A. (1994) Summary: the modified nucleosides in RNA. *Nucleic Acids Res.*, **22**, 2183–2196.
3. Cantara,W.A., Crain,P.F., Rozenski,J., McCloskey,J.A., Harris,K.A., Zhang,X., Vendeix,F.A.P., Fabris,D. and Agris,P.F. (2011) The RNA Modification Database, RNAMDB: 2011 update. *Nucleic Acids Res.*, **39**, 195–201.
4. Motorin,Y. and Helm,M. (2011) RNA nucleotide methylation. *Wiley Interdiscip. Rev. RNA*, **2**, 611–631.
5. Maden,B.E. (1990) The numerous modified nucleotides in eukaryotic ribosomal RNA. *Prog. Nucleic Acid Res. Mol. Biol.*, **39**, 241–303.
6. Piekna-Przybylska,D., Decatur,W.A. and Fournier,M.J. (2008) The 3D rRNA modification maps database: with interactive tools for ribosome analysis. *Nucleic Acids Res.*, **36**, 178–183.
7. Bachellerie,J.P., Cavaille,J. and Hüttenhofer,A. (2002) The expanding snoRNA world. *Biochimie*, **84**, 775–790.
8. Decatur,W.A. and Fournier,M.J. (2002) rRNA modifications and ribosome function. *Trends Biochem. Sci.*, **27**, 344–351.
9. Xue,S. and Barna,M. (2012) Specialized ribosomes: a new frontier in gene regulation and organismal biology. *Nat. Rev. Mol Cell Biol.*, **13**, 355–369.
10. Marcel,V., Ghayad,S.E., Belin,S., Therizols,G., Morel,A.P., Solano-Gonzàlez,E., Vendrell,J.A., Hacot,S., Mertani,H.C., Albaret,M.A. *et al.* (2013) p53 acts as a safeguard of translational control by regulating fibrillarin and rRNA methylation in cancer. *Cancer Cell*, **24**, 318–330.
11. Gonzales,B., Henning,D., So,R.B., Dixon,J., Dixon,M.J. and Valdez,B.C. (2005) The Treacher Collins syndrome (TCOF1) gene product is involved in pre-rRNA methylation. *Hum. Mol. Genet.*, **14**, 2035–2043.
12. Stepanov,G.A., Filippova,J.A., Komissarov,A.B., Kuligina,E.V., Richter,V.A. and Semenov,D.V. (2015) Regulatory role of small nucleolar RNAs in human diseases. *Biomed. Res. Int.*, 10.1155/2015/206849.
13. Karijolich,J. and Yu,Y.T. (2010) Spliceosomal snRNA modifications and their function. *RNA Biol.*, **7**, 192–204.
14. Cavaillé,J., Buiting,K., Kiefmann,M., Lalande,M., Brannan,C.L., Horsthemke,B., Bachellerie,J.P., Brosius,J. and Hüttenhofer,A. (2000)

Identification of brain-specific and imprinted small nucleolar RNA genes exhibiting an unusual genomic organization. *Proc. Natl. Acad. Sci. U.S.A.*, **97**, 14311–14316.
15. Dönmez,G., Hartmuth,K. and Lührmann,R. (2004) Modified nucleotides at the 5′ end of human U2 snRNA are required for spliceosomal E-complex formation. *RNA*, **10**, 1925–1933.
16. Popova,A.M. and Williamson,J.R. (2014) Quantitative analysis of rRNA modifications using stable isotope labeling and mass spectrometry. *J. Am. Chem. Soc.*, **136**, 2058–2069.
17. Kellner,S., Burhenne,J. and Helm,M. (2010) Detection of RNA modifications. *RNA Biol.*, **7**, 237–247.
18. Grosjean,H., Droogmans,L., Roovers,M. and Keith,G. (2007) Detection of enzymatic activity of transfer RNA modification enzymes using radiolabeled tRNA substrates. *Methods Enzymol.*, **425**, 55–101.
19. Birkedal,U., Christensen-Dalsgaard,M., Krogh,N., Sabarinathan,R., Gorodkin,J. and Nielsen,H. (2015) Profiling of ribose methylations in RNA by high-throughput sequencing. *Angew. Chem. Int. Ed.*, **54**, 451–455.
20. Yu,Y.T., Shu,M.D. and Steitz,J.A. (1997) A new method for detecting sites of 2′-O-methylation in RNA molecules. *RNA*, **3**, 324–331.
21. Buchhaupt,M., Peifer,C. and Entian,K.D. (2007) Analysis of 2‘-O-methylated nucleosides and pseudouridines in ribosomal RNAs using DNAzymes. *Anal. Biochem.*, **361**, 102–108.
22. Motorin,Y., Muller,S., Behm-Ansmant,I. and Branlant,C. (2007) Identification of modified residues in RNAs by reverse transcription-based methods. *Methods Enzymol.*, **425**, 21–53.
23. Higa-Nakamine,S., Suzuki,T., Uechi,T., Chakraborty,A., Nakajima,Y., Nakamura,M., Hirano,N., Suzuki,T. and Kenmochi,N. (2012) Loss of ribosomal RNA modification causes developmental defects in zebrafish. *Nucleic Acids Res.*, **40**, 391–398.
24. Blatter,N., Bergen,K., Nolte,O., Welte,W., Diederichs,K., Mayer,J, Wieland,M. and Marx,A. (2013) Structure and function of an RNA-reading thermostable DNA polymerase. *Angew. Chem. Int. Ed.*, **52**, 11935–11939.
25. Gloeckner,C., Kranaster,R. and Marx,A. (2010) Directed evolution of DNA polymerases: construction and screening of DNA polymerase mutant libraries. *Curr. Protoc. Chem. Biol.*, **2**, 89–109.
26. Jaeger,S. (2003) Patent US20030165982 A1.
27. Rudinger,N.Z., Kranaster,R. and Marx,A. (2007) Hydrophobic amino acid and single-atom substitutions increase DNA polymerase selectivity. *Chem. Biol.*, **14**, 185–194.
28. Pfaffl,M.W. (2001) A new mathematical model for relative quantification in real-time RT-PCR. *Nucleic Acids Res.*, **29**, e45.
29. Buchhaupt,M., Sharma,S., Kellner,S., Oswald,S., Paetzold,M., Pfeifer,C., Watzinger,P., Schrader,J., Helm,M. and Entian,K.D. (2014) Partial methylation at Am100 in 18s rRNA of baker’s yeast reveals ribosome heterogeneity on the level of eukaryotic rRNA modification. *PLoS One*, **9**, e89640.
30. Li,Y., Korolev,S. and Waksman,G. (1998) Crystal structures of open and closed forms of binary and ternary complexes of the large fragment of Thermus aquaticus DNA polymerase I: structural basis for nucleotide incorporation. *EMBO J.*, **17**, 7514–7525.
31. Aschenbrenner,J., Drum,M., Topal,H., Wieland,M. and Marx,A. (2014) Direct sensing of 5-methylcytosine by polymerase chain reaction. *Angew. Chem. Int. Ed.*, **53**, 8154–8158.
32. Harcourt,E.M., Ehrenschwender,T., Batista,P.J., Chang,H.Y. and Kool,E.T. (2013) Identification of a selective polymerase enables detection of N(6)-methyladenosine in RNA. *J. Am. Chem. Soc.*, **135**, 19079–19082.
33. He,C. (2010) Grand challenge commentary: RNA epigenetics? *Nat. Chem. Biol.*, **6**, 863–865.